Available online at www.sciencedirect.com
SCIENCE DIRECT®
Journal of Organometallic Chemistry 690 (2005) 5206–5214
Journal of Organometallic Chemistry
www.elsevier.com/locate/jorganchem

Catalytic hydrogenolysis of alkyl halides by sulfido-bridged molybdenum clusters: A density functional study

John E. McGrady *, José Gracia

Department of Chemistry, University of York, Heslington, York YO10 5DD, United Kingdom

Received 13 February 2005; received in revised form 6 April 2005; accepted 6 April 2005
Available online 31 May 2005

Abstract

Density functional theory has been used to explore the mechanism of cleavage of H_2 at a sulfido-bridged molybdenum cluster, CpMo(μ-SH)(μ-S)(μ-S_2CH_2)MoCp. The addition occurs across a single Mo–S bond, and the disruption of the strong Mo–S π bonding in the ground state leads to a very high-lying transition state (+43 kcal mol^{-1}). Once formed, the adsorbed hydrogen migrates over the cluster via a series of hops from metal to sulphur, formally corresponding to a switch from hydridic to protic character. The low barrier (+15 kcal mol^{-1}) for migration leads to facile hydrogenolysis of coordinated substrates.

Keywords: Density functional theory; Hydrogen activation; Sulfide clusters

1. Introduction

In a recent publication [1], we explored the role of a thiolato-bridged dimolybdenum core (Scheme 1(a)) in the electrochemical reduction of a coordinated phenyldiazene (PhN=NH) ligand [2]. In this reaction, the bimetallic unit proves to be much more than a passive support for the intermediates – it also plays a key role as a source of electrons that can be transferred reversibly to the coordinated substrate. Most significantly, only the highest occupied molecular orbital on the dimolybdenum core is active in the reduction process, and its shape exerts a controlling influence on the reaction pathway. Electrochemical reduction processes such as this have clear links to many biological redox processes, where electrons and protons are often delivered separately to the substrate. An alternative strategy, more familiar to synthetic organometallic chemists, is to utilise molecular hydrogen as the primary reductant, perhaps the best studied examples being the molybdenum sulfide-catalysed hydrogenolysis reactions [3] involved in the hydrodesulfurisation of organosulfur compounds [4]. It is generally acknowledged in these cases that the molybdenum sulfide surface is the catalytic site for the hydrogenolysis reaction, but, as with the majority of heterogeneous systems, attempts to elucidate precise mechanistic details are hampered by the ill-defined nature of the catalytic species [5]. A number of chemists have therefore turned to well-defined Mo/S-based molecular analogues to probe the mechanism of hydrogenolysis. Rakowski DuBois and co-workers [6] have been prominent in this respect, conducting a number of investigations into the catalytic activity of sulfido-bridged dimolybdenum species (for example, that shown in Scheme 1(b)). In a series of papers, a diverse range of catalytic hydrogen activation processes has been explored, including H/D scrambling in H_2/D_2 mixtures [7], hydrogenolysis of organic halides [8] and the reduction of unsaturated hydrocarbons [9] and nitrogenous substrates such as azobenzene (PhN=NPh) [7c,10]. The sulfido-bridged dimolybdenum

* Corresponding author. Tel.: +44 1904 434539; fax: +44 1904 432516
E-mail address: jem15@york.ac.uk (J.E. McGrady).

0022-328X/$ - see front matter © 2005 Elsevier B.V. All rights reserved.
doi:10.1016/j.jorganchem.2005.04.004

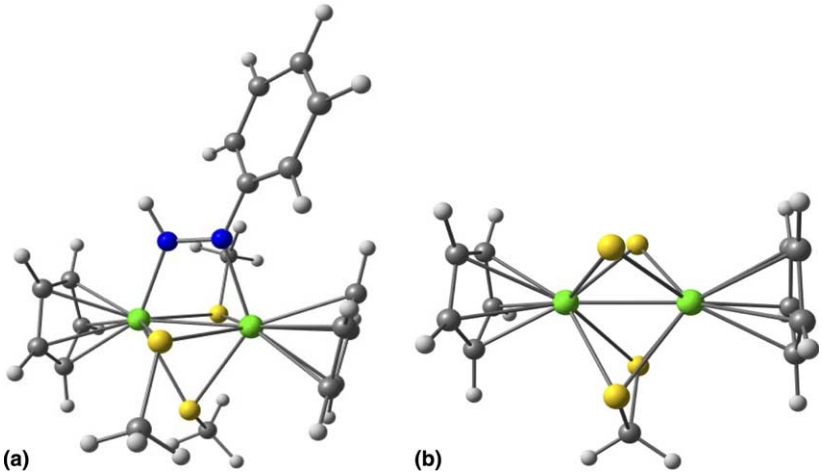

Scheme 1. Structures of the thiolato-bridged dimolybdenum cores involved in (a) electrochemical reduction of phenyldiazene and (b) hydrogenolysis of alkyl halides.

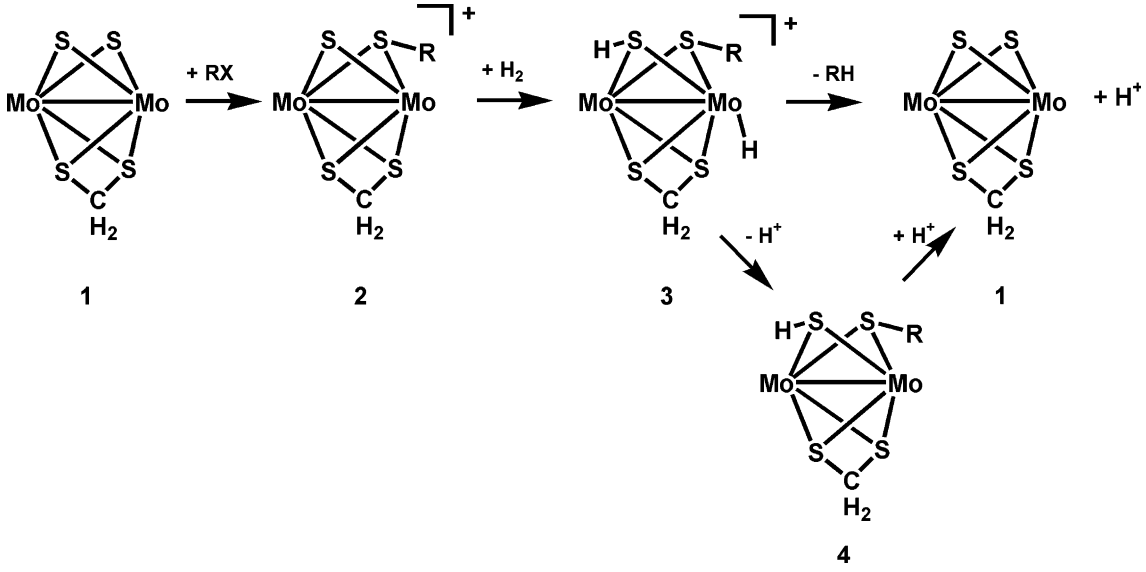

Scheme 2. Proposed mechanism for catalytic hydrogenolysis of RX by $(CpMo)_2(\mu\text{-}S_2CH_2)(\mu\text{-}S)_2$ [6].

core is common to both molecules shown in Scheme 1, and, in an interesting parallel to the work described in the first paragraph [1,2], polymer supported analogues of (**b**) are also able to electrocatalyse the reduction of N=N double bonds [11]. In this contribution, we use density functional theory to explore perhaps the simplest of the catalytic hydrogen activation processes, the hydrogenolysis of organo-halides by the molybdenum (IV) sulfide complex $(CpMo)_2(\mu\text{-}S_2CH_2)(\mu\text{-}S)_2$ (**1**) (Scheme 1(b)) [6,8].

On the basis of their experimental work, Rakowski DuBois and co-workers [6,8] have made a number of mechanistic proposals that we use as a framework for this paper (Scheme 2). Under relatively mild conditions (343 K, 1–2 atm H_2), the hydrogenolysis of, for example, β-bromo styrene proceeds slowly, allowing for the isolation and identification of intermediates. The hydrogenolysis is proposed to occur via initial nucleophilic attack of a sulfido-ligand on the alkyl halide, yielding the cationic species $[(CpMo)_2(\mu\text{-}S_2CH_2)(\mu\text{-}S)(\mu\text{-}SR)]^+$ (**2**). The exact mechanism of hydrogen cleavage by **2** is uncertain, although the activation parameters are consistent with a bimolecular interaction between catalyst and H_2 [8a]. Two distinct routes for transition metal-mediated H–H bond cleavage are known, homolytic and heterolytic [12], the former being predominant in electron-rich metal complexes, the latter in more electrophilic species. A very recent study of the hydrogenation of a sulfido-bridged Ir^{II} species has in fact revealed that both mechanisms are operative, homolytic cleavage of one H–H bond being followed by a second heterolytic step [13]. In the case of H_2 activation by **2**, heterolytic cleavage, leading to the hydridic intermediate $(CpMoH)(\mu\text{-}S_2CH_2)(\mu\text{-}SH)(\mu\text{-}SR)(MoCp)]^+$ (**3**), has

been proposed as the most likely route, consistent with the high metal oxidation states (Mo^{IV}). For electron-withdrawing R groups, elimination of R–H from **3** leads to starting material, **1**, plus proton. In the presence of base, the reaction takes a different pathway, giving the stable species $(CpMo)_2(\mu\text{-}S_2CH_2)(\mu\text{-}SH)(\mu\text{-}SR)$ (**4**), presumably through deprotonation of **3**. Re-acidification of **4** generates H_2 rather than R–H [10a], but the corresponding reaction with the dialkylated analogues, $(CpMo)_2(\mu\text{-}S_2CH_2)(\mu\text{-}SR)(\mu\text{-}SR)$ does lead to elimination of the hydrocarbon, supporting the proposal that intermediates such as **3** participate in the hydrogenolysis reaction.

In the course of this theoretical study, we aim to establish whether the fundamental electronic principles developed for separate electron/proton transfer are applicable to reduction processes using molecular hydrogen. Extended Hückel theory has already been used to provide some insight into the electronic structure of these and related sulfido-bridged bimetallic species [14]. More recently, density functional theory has been used to analyse structural problems in metal sulfide chemistry [15], and the role of these species in both biological [16,17] and non-biological reduction processes [18]. Our theoretical approach to this problem involves the full characterisation of the potential energy surface for hydrogenolysis using the prototype reaction where R = H, in which case the elimination of product is simply the microscopic reverse of the initial H_2 activation process. Although the replacement of R with H will undoubtedly affect the basicity of the thiolate ligands, we are confident that the basic features of the potential energy surface will be accurately reproduced. Through this approach, we aim to identify the site of H_2 activation, and understand the nature of the electronic redistribution that occurs within the bimetallic unit upon reduction.

1.1. Computational details

All calculations are based on density functional theory [19,20], performed using the GAUSSIAN 03 programme [21]. In all cases, the B3LYP functional was used [22], along with the LANL2DZ [23] basis set and its associated effective core potential for Mo and S, augmented by a set of f and d polarisation functions, respectively [24,25]. The 6-31G(d,p) basis set was used for all other atoms. The nature of all transition states and minima was confirmed by the presence of one or zero imaginary frequencies, respectively.

1.2. Electronic structure of $[(CpMo)_2(\mu\text{-}S_2CH_2)(\mu\text{-}S)_2]$ (**1**), and $[(CpMo)_2(\mu\text{-}S_2CH_2)(\mu\text{-}S)(\mu\text{-}SH)]^+$ (**2**)

As noted in the introduction, the initial step in the hydrogenolysis reaction is nucleophilic attack by a bridging sulfide ligand of $[(CpMo)_2(\mu\text{-}S_2CH_2)(\mu\text{-}S)_2]$ (**1**), on an alkyl halide, R–X (R = H in our prototype reaction). The electronic structure of **1** and its protonated derivative, **2**, therefore represent a logical starting point for the discussion. The optimised structures of the two complexes are summarised in Fig. 1, along with their frontier molecular orbital arrays. The Mo–Mo and Mo–S bond lengths of 2.62, 2.31 and 2.53 Å in **2** are very similar to the corresponding crystallographically determined values of 2.608(1), 2.301(1) and 2.484(1) Å in the analogous thiophene species $[(MeCpMo)_2(\mu\text{-}S_2CH_2)(\mu\text{-}S)(\mu\text{-}S\text{-}C_4H_3S)]^+$ [8]. In both **1** and **2**, the formal oxidation state of the Mo_2 core is $Mo^{IV}Mo^{IV}$, and two occupied metal-based orbitals, one with Mo–Mo σ symmetry, the other δ^*, are clearly identifiable in the frontier region in each case. Strong Mo–S π interactions are apparent in the LUMOs of both species (66a, Mo–S π^*). Protonation reduces the symmetry, and strongly stabilises one of the sulfur-based lone pair orbitals, but does not significantly alter the energies or distributions of the metal-based orbitals. The Mo–Mo bond length is consequently largely unaffected, despite the 0.16 Å increase in the length of the protonated Mo–S bonds. The structural and electronic integrity of the bimetallic core was highlighted as a key feature in our previous work on the reduction of phenyldiazene, and it seems that the $Mo(\mu\text{-}S_2CH_2)(\mu\text{-}S)(\mu\text{-}SR)Mo$ core has similar properties.

1.3. Hydrogen activation by $[(CpMo)_2(\mu\text{-}S_2CH_2)(\mu\text{-}S)(\mu\text{-}SH)]^+$ (**2**)

The structures of stationary points located on the potential energy surface for $[(CpMo)_2(\mu\text{-}S_2CH_2)(\mu\text{-}S)(\mu\text{-}SH)]^+$ (**2**), $+H_2$ are summarised in Fig. 2. We have considered a number of possible structures for intermediate **3** (**3**$_{a–e}$), the product of H_2 binding. For structure **3**$_a$, formally a $Mo^{V}Mo^{III}$ hydride species, there are in fact seven distinct minima, differing only in the relative conformations of the hydride ligand and the thiolate hydrogens. All seven lie within 3 kcal mol^{-1}, and are structurally very similar, so only the three (**3**$_a$, **3**$'_a$ and **3**$''_a$) that are important to the subsequent discussion of the hydrogenolysis pathway are shown in Fig. 2. The presence of a hydride ligand in structures **3**$_a$, **3**$'_a$ and **3**$''_a$ has remarkably little impact on the coordination sphere of the molybdenum centre, resulting only in a slight displacement of the Cp ring, but the protonation of the sulfido ligand causes a significant lengthening of the Mo–S bonds (2.31 Å in **2** to 2.53 Å in **3**$_a$). Two distinct transition states, **TS1** and **TS1′**, linking **2** + H_2 with **3**$_a$ and **3**$''_a$, respectively, have been located approximately 43 kcal mol^{-1} above the separated reactants (Fig. 3). The two transition states differ only in the orientation of the H_2 molecule relative to the bridging sulfido ligand (Scheme 3). Whilst the large calculated

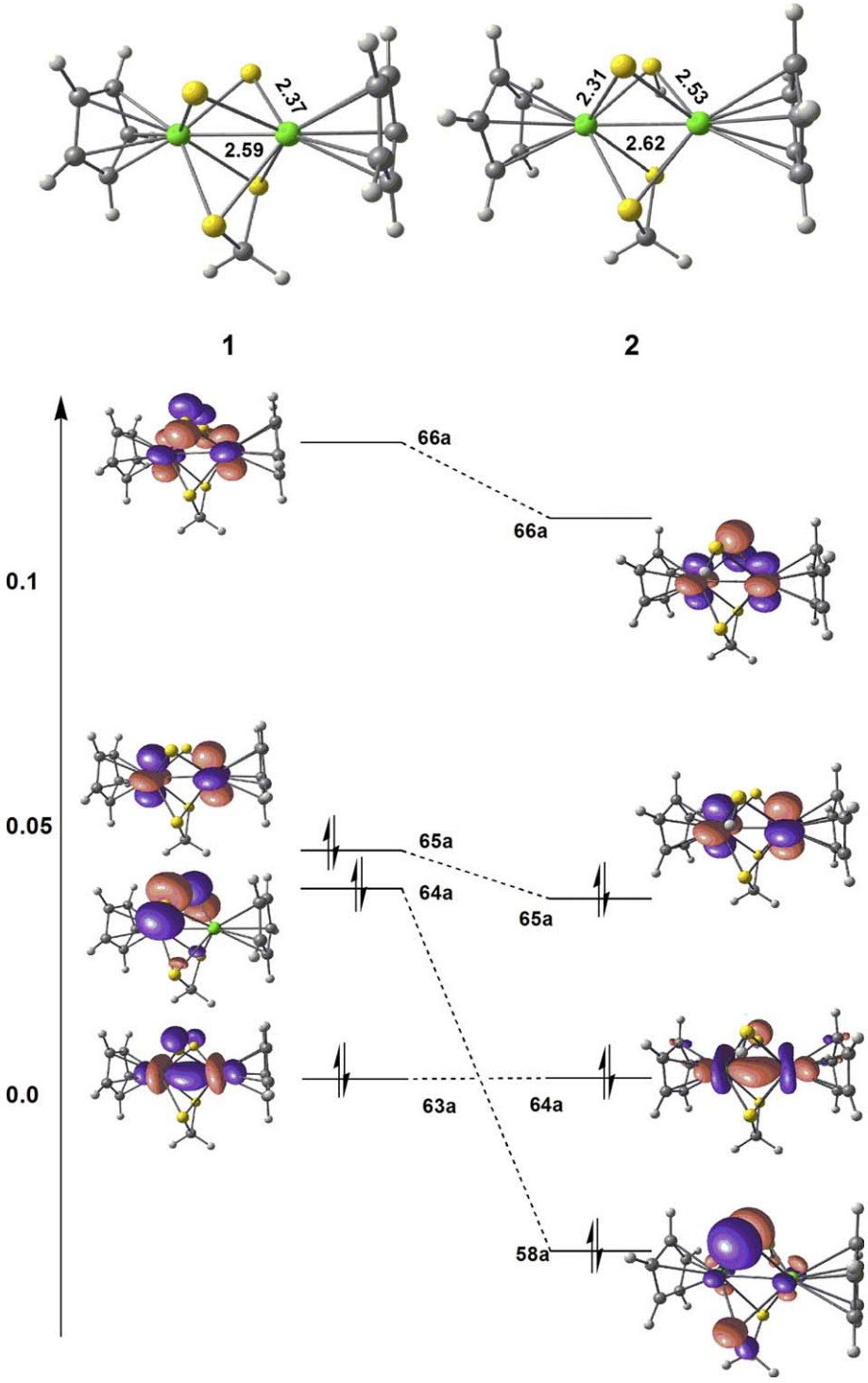

Fig. 1. Optimised structures and frontier orbitals for **1** and **2**.

barrier is fully consistent with the slow rate of reaction observed experimentally, we note that it is almost an order of magnitude higher than the value of 7.2 kcal mol^{-1} reported by Mealli and co-workers [18] for the rhodium species $[(triphos)Rh(\mu\text{-}S)_2Rh(triphos)]^{2+}$. The origin of the dramatic difference between the two systems can be traced to two distinct factors. The first is that in the rhodium system (and also in the hydrogenase enzymes) [16], heterolytic cleavage is preceded by the formation of an η^2-H_2 complex, and so the Rh–H bond is already well formed at the transition state (1.69 vs. 2.13 Å in **TS1**). We have been unable to locate any equivalent η^2-H_2 complex on the potential energy surface for **3**, probably due to the lack of a vacant coordination site

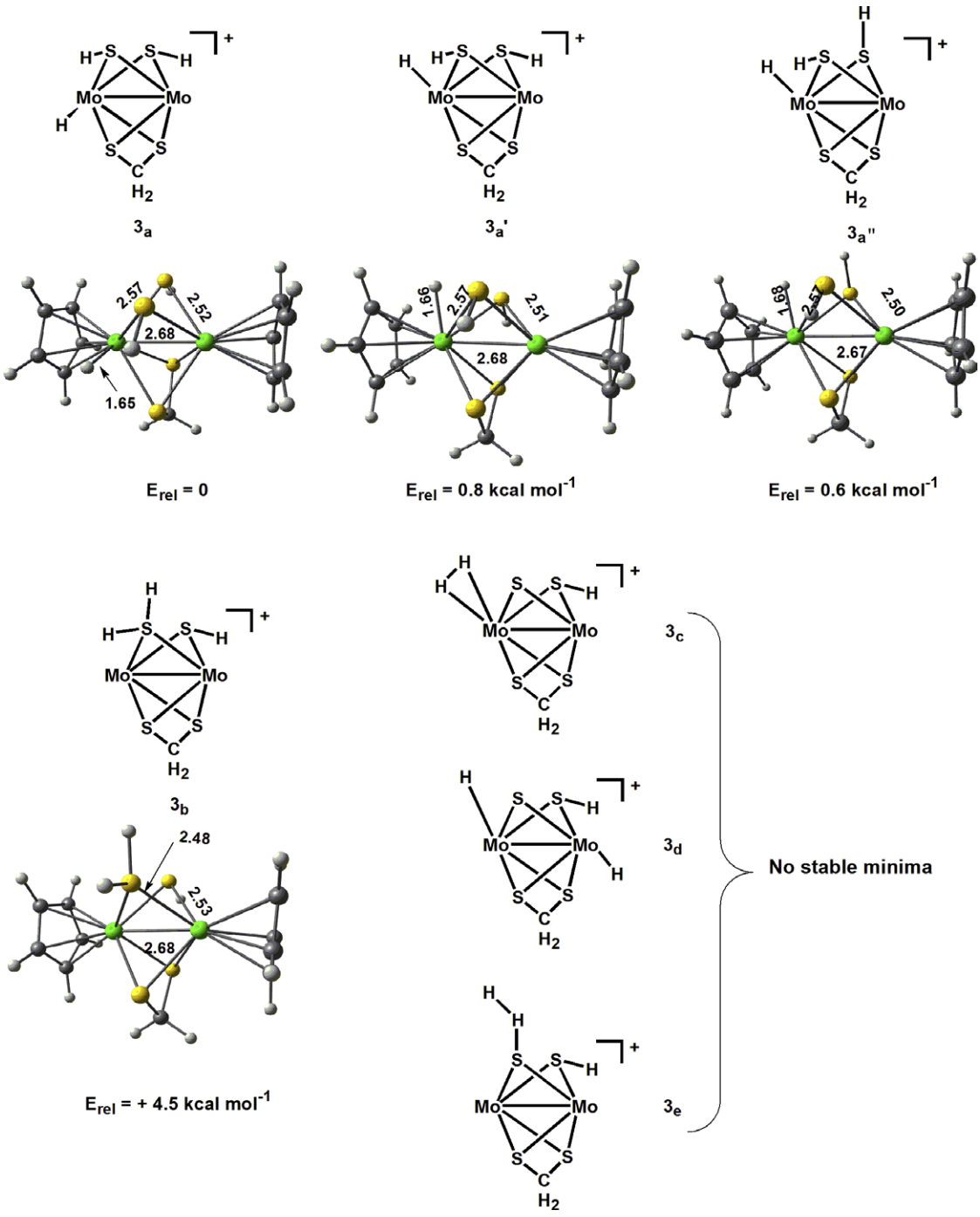

Fig. 2. Optimised structures of isomers of $[(CpMo)_2(\mu\text{-}S_2CH_2)(\mu\text{-}S)(\mu\text{-}SH)(H_2)]^+$ (**3**).

in **2** and the relative electron deficiency of the Mo^{IV} centres. The second factor is the very different nature of the Mo–S and Rh–S bonds. In the rhodium case, the d^6 configuration of the Rh^{III} centres precludes effective π interactions, and the Rh–S bond length increases only from 2.40 Å in $[(triphos)Rh(\mu\text{-}S)_2Rh(triphos)]^{2+}$ to 2.54 Å in the transition state [18]. In contrast, the highly electron-deficient Mo^{IV} centres (d^2) in **2** are strongly stabilised by Mo–S π bonding which is disrupted in the transition state, as a result of which, the Mo–S bond length increases from 2.31 Å in **2** to 2.63 Å in **TS1/TS1′**. The strong Mo–S π bonding in **2** is also responsible for the overall endothermicity of the H_2 heterolysis (+5.3 kcal mol^{-1}) compared to the exothermic reaction ($\Delta E = -17$ kcal mol^{-1}) for $[(triphos)Rh(\mu\text{-}S)_2Rh(triphos)]^{2+}$.

A second isomer, structure $\mathbf{3_b}$, corresponding formally to a $Mo^{III}Mo^{III}$ species with bridging thiolato (SH^-) and mercaptan (SH_2) ligands was also located 4.5 kcal mol^{-1} above $\mathbf{3_a}$, indicating a significant prefer-

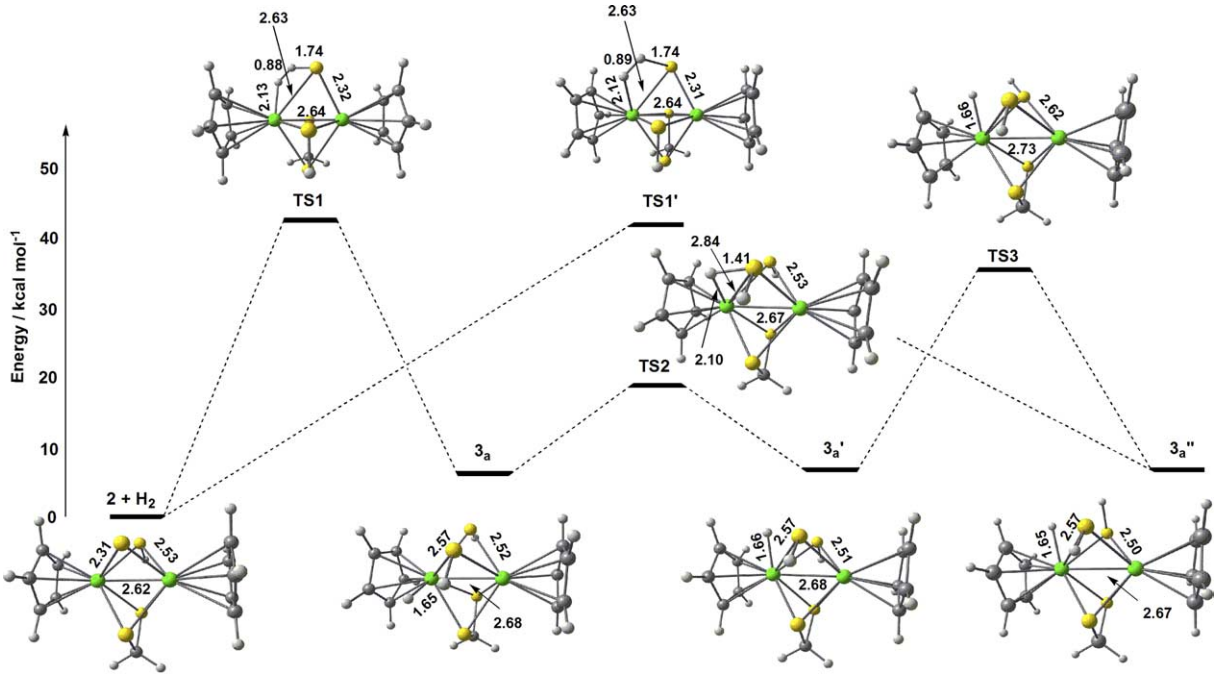

Fig. 3. Structures and relative energies for stationary points on the potential energy surface of $[(CpMo)_2(\mu\text{-}S_2CH_2)(\mu\text{-}S)(\mu\text{-}SH)(H_2)]^+$ (**3**).

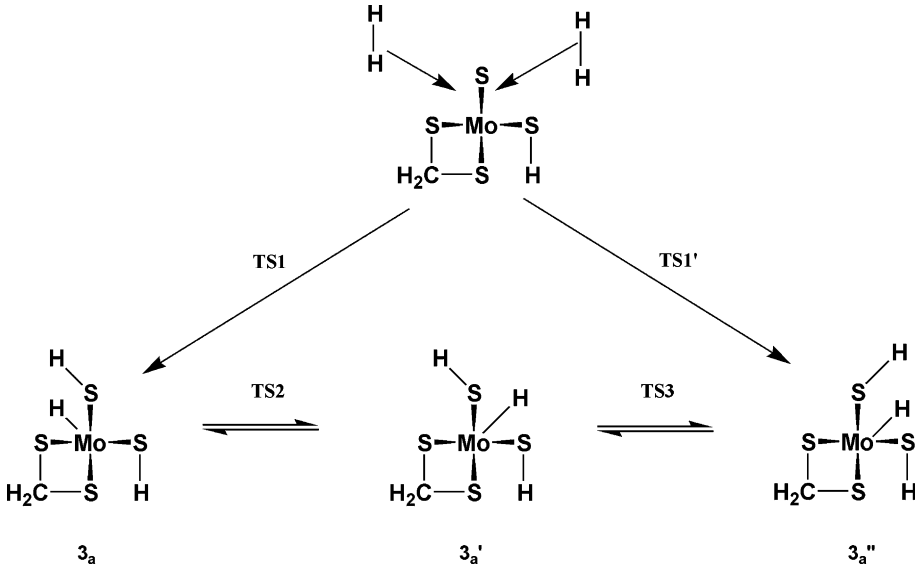

Scheme 3. Formation and rearrangement pathways for isomers of $\mathbf{3_a}$.

ence for heterolytic ($\mathbf{3_a}$) over homolytic ($\mathbf{3_b}$) fission, consistent with the original mechanistic proposal [8a]. The separation between $\mathbf{3_a}$ and $\mathbf{3_b}$ is, however, comparatively small, suggesting that conversion from hydridic ($\mathbf{3_a}$) to protic ($\mathbf{3_b}$) character is relatively facile. In the following section, we will argue that the energetic accessibility of this type of interconversion plays a key role in the mobility of adsorbed hydrogen atoms on the cluster. Finally, we note that we find no evidence for either a dihydride species $\mathbf{3_d}$, or an end-on η^2-H_2 complex, $\mathbf{3_e}$, both of which have been proposed previously: all attempts to optimise a dihydride lead instead to $\mathbf{3_a}$, while all end-on structures resulted in the dissociation of H_2.

1.4. Rearrangement of the intermediates: hydride migration

Following heterolytic cleavage of the H–H bond, the ultimate elimination of R–H (or H–H in our simplified model system) requires the migration of the hydride ligand and/or the R group such that the two lie in a *cisoid* arrangement with respect to a Mo–S bond, and it is

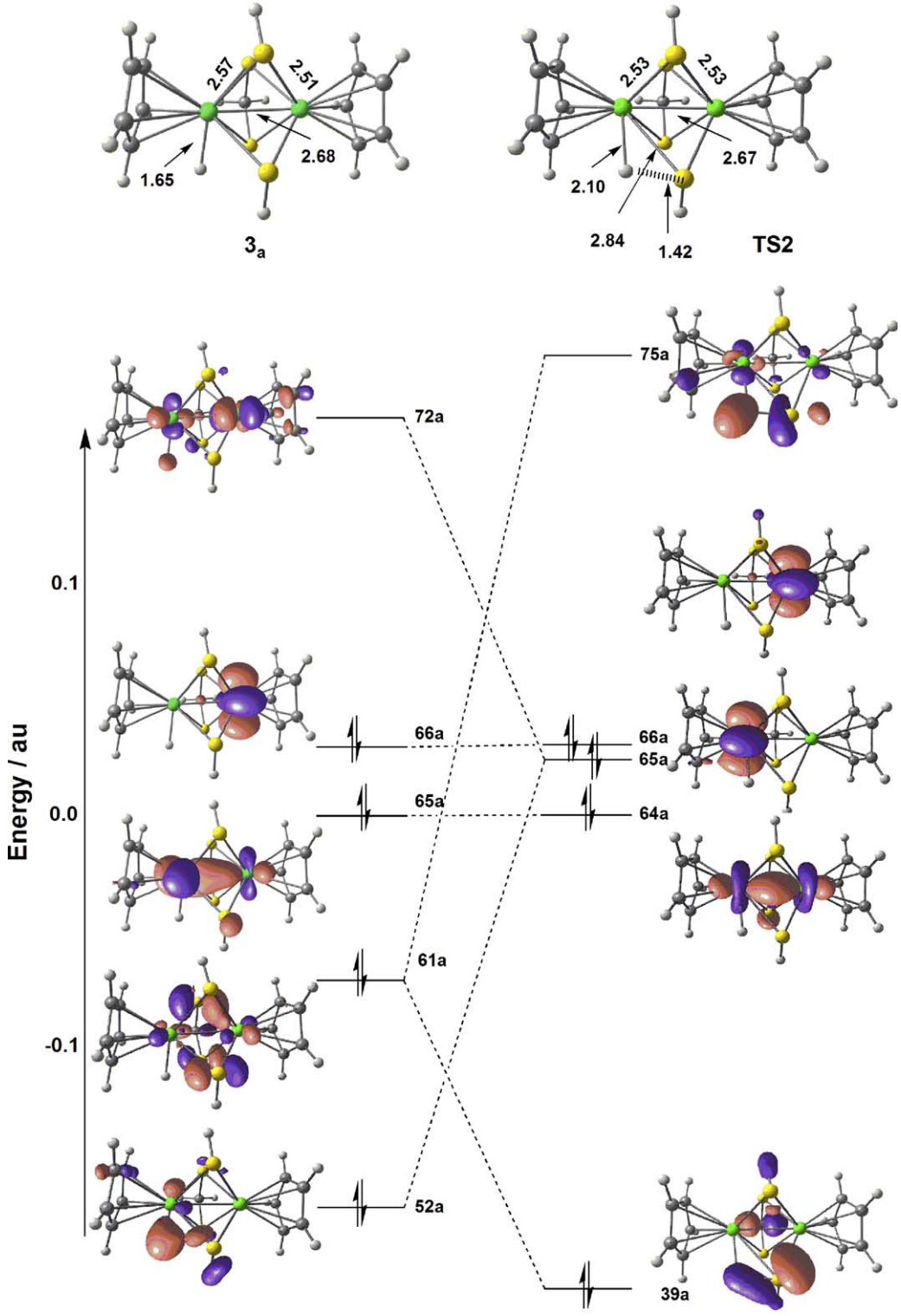

Fig. 4. Frontier orbitals for $\mathbf{3_a}$ and **TS2**, showing the evolution of the metal, hydrogen and sulfur-based orbitals as the hydrogen migrates around the cluster.

clearly important to establish whether this rearrangement could be rate-limiting. The migration of the hydride from one side of the cluster to the other involves a 180° rotation about the Mo–Mo axis, and must therefore proceed via $\mathbf{3'_a}$, where the hydride bisects the two bridging –SH ligands. A transition state, **TS2**, connecting $\mathbf{3_a}$ and $\mathbf{3'_a}$ has been located only 13.4 kcal mol^{-1} above $\mathbf{3_a}$ and almost 30 kcal mol^{-1} below **TS1**, indicat-

ing that, once formed, the hydride is relatively mobile on the cluster surface. From $\mathbf{3}'_{\mathbf{a}}$, the necessary *cisoid* arrangement of hydride and thiolate proton can be achieved by a further rotation of the hydride ligand which, in our symmetric model system, is simply the mirror image of the $\mathbf{3_a} \rightarrow \mathbf{TS2} \rightarrow \mathbf{3}'_{\mathbf{a}}$ process. Alternatively, an inversion at the thiolate sulfur, via **TS3**, can convert $\mathbf{3}'_{\mathbf{a}}$ into $\mathbf{3}''_{\mathbf{a}}$, from where elimination could occur via **TS1′**. **TS3**, however, lies some 17 kcal mol^{-1} above **TS2**, suggesting that hydride migration rather than sulfide inversion will be the dominant mechanism for interconverting the various isomers of $\mathbf{3_a}$. In any case, both **TS2** and **TS3** lie significantly below **TS1** and **TS1′**, confirming that the heterolysis of the H–H bond is rate limiting.

The structure of **TS2** has a number of features that suggest a distinct shift in electronic structure compared to either $\mathbf{3_a}$ or $\mathbf{3}'_{\mathbf{a}}$: in particular, the Mo–H bond is lengthened by almost 0.5 Å relative to either of the hydride species (2.10 vs. 1.65 Å), while the S···H separation is reduced to 1.42 Å, close to the bonding distance of ~1.35 Å. The separation between the Mo centre carrying the hydride ligand and the bridging sulfur atom also increases dramatically to 2.81 Å. Comparison of the frontier orbital domains of $\mathbf{3_a}$ and **TS2** (Fig. 4) reveals the origins of these structural trends. The hydride, $\mathbf{3_a}$, is formally a $Mo^{V}Mo^{III}$ species, with two occupied metal-based orbitals, the HOMO (66a) and HOMO-1 (65a), the former localised entirely on a single centre (Mo^{III}), the latter delocalised over both. The metal-hydride bonding and antibonding orbitals, 52a and 72a, respectively, formed by a combination of Mo $4d_{xy}$ and hydrogen 1s, are also shown in the Figure. The motion of the hydride along the reaction coordinate ($\mathbf{3a} \rightarrow \mathbf{TS2}$) takes it onto a node on the d_{xy} orbital, and the Mo–H bonding/antibonding pair (52a/72a) collapses to a single non-bonding orbital (65a in **TS2**). At the same time, overlap of the 1s orbital on the hydrogen with the lone pair of the bridging thiolato ligand (61a in $\mathbf{3}_{\mathrm{a}}$) increases, leading to the formation of new S-H bonding/antibonding pair, 39a/75a in **TS2**. The orbital array for **TS2** is in fact more consistent with a $Mo^{III}Mo^{III}$ oxidation state, with three distinct metal-based orbitals in the occupied domain (64a, 65a and 66a). In this context, it is interesting to note the structural similarities between **TS2** and the unambiguously $Mo^{III}Mo^{III}$ species discussed previously, intermediate, $\mathbf{3_b}$ (the only significant difference between **TS2** and $\mathbf{3_b}$ is the orientation of the H_2S group relative to the Mo–Mo axis). The comparison between intermediate $\mathbf{3_b}$ and **TS2** clearly illustrates the role of the bridging thiolato ligand as an internal base [8b]. Thus, although the migration of the hydrogen atom can formally be described as a series of hydride ($\mathbf{3_a}$ and $\mathbf{3}'_{\mathbf{a}}$) to proton (**TS2**) shifts, the evolution of the frontier orbitals suggests that a more realistic picture is of a proton migrating over a continuous cloud of non-bonding electron density contained in the metal d orbitals ($\mathbf{3_a}$ and $\mathbf{3}'_{\mathbf{a}}$) and the sulfur lone pair (**TS2**). The very low barrier for the migration, first hinted at by the energetic proximity of the two minima, $\mathbf{3_a}$ and $\mathbf{3_b}$, suggests that highly mobile adsorbed hydrogen atoms are likely to be a general feature of Mo/S-based cluster catalysis.

2. Summary

A detailed survey of the potential energy surface for H_2 addition and elimination to $[(CpMo)_2(\mu\text{-}S_2CH_2)(\mu\text{-}S)(\mu\text{-}SH)]^+$ has revealed a number of features of potential relevance to the catalytic process. Most strikingly, the metal core itself is remarkably stable throughout the cycle, the Mo–Mo separation changing by only 0.05 Å despite fluctuations in formal oxidation state from $Mo^{IV}Mo^{IV}$ to $Mo^{V}Mo^{III}$ and $Mo^{III}Mo^{III}$. The origin of this stability can be traced to the splitting of the metal-based manifold into a strongly bonding σ orbital and a pair of essentially non-bonding δ symmetry orbitals. All intramolecular electron transfer from metal to H_2 involves the δ manifold, leaving the σ electron density unperturbed, and the strong Mo–Mo σ bond maintains the integrity of the bimetallic structure, even in circumstances where one of the bridging ligands is almost completely dissociated. Following H–H bond activation, the adsorbed hydrogen can migrate around the Mo–Mo axis with relative ease in a process that corresponds to a series of hops from hydridic to protic sites. The evolution of the frontier orbitals, however, suggests that a more physically realistic picture is of a proton migrating over a continuous cloud of electron density formed by the metal-based d orbitals and the sulfur-based lone pairs. The latter viewpoint is consistent both with the low barrier to migration, and also the well-known acidity of this and other metal hydrides.

Acknowledgement

J.G.B. acknowledges the EU for a fellowship under the Marie Curie Host Fellowship programme.

References

[1] J.K. Padden Metzker, J.E. McGrady, Chem. Eur. J 10 (2004) 6447.
[2] N. Le Grand, K.W. Muir, F.Y. Petillon, C.J. Pickett, P. Schollhammer, J. Talarmin, Chem. Eur. J. 8 (2002) 3115.
[3] O. Weisser, S. Landa, Sulphide Catalysts, Their Properties and Applications, Pergamon Press, Oxford, 1973.
[4] (a) B.C. Gates, J.R. Katzer, G.C.A. Schuit, The Chemistry of Catalytic Processes, McGraw-Hill, New York, 1979, p. 422;
(b) J. Barbow, K.C. Campbell, J. Chem. Soc., Chem. Commun. (1982) 1371;

(c) F.E. Massoth, Adv. Catal. 27 (1978) 265;
(d) S.C. Schuman, H. Shalit, Catal. Rev. 4 (1970) 245;
(e) D.E. Schwarz, J.A. Dopke, T.B. Rauchfuss, S.R. Wilson, Angew. Chem., Int. Ed. Engl. 40 (2001) 2351.
[5] (a) D.R. Kilanowski, H. Teeuwen, V.H.J. de Beer, B.C. Gates, G.C.A. Schuit, H. Kwart, J. Catal. 55 (1978) 129;
(b) H. Kwart, G.C.A. Schuit, B.C. Gates, J. Catal. 61 (1980) 128.
[6] (a) M. Rakowski DuBois, Chem. Rev. 89 (1989) 1;
(b) M. Rakowski DuBois, in: R.D. Adams, F.A. Cotton (Eds.), Catalysis by Di- and Polynuclear Metal Cluster Complexes, Wiley, 1998.
[7] (a) M. Rakowski DuBois, M.C. VanDerveer, D.C. DuBois, R.C. Haltiwanger, W.K. Miller, J. Am. Chem. Soc. 102 (1980) 7456;
(b) L.L. Lopez, G. Godziela, M. Rakowski DuBois, Organometallics 10 (1991) 2660;
(c) C.J. Casewit, D.E. Coons, L.L. Wright, W.K. Miller, M. Rakowski DuBois, Organometallics 5 (1986) 951.
[8] (a) L.L. Lopez, P. Bernatis, J. Birnbaum, R.C. Haltiwanger, M. Rakowski DuBois, Organometallics 11 (1992) 2424;
(b) P. Bernatis, R.C. Haltiwanger, M. Rakowski DuBois, Organometallics 11 (1992) 2435;
(c) D.E. Coons, R.C. Haltwinger, M. Rakowski DuBois, Organometallics 6 (1987) 2417;
(d) R.T. Weberg, R.C. Haltiwanger, J.C.V. Laurie, M. Rakowski DuBois, J. Am. Chem. Soc. 108 (1986) 6242.
[9] (a) M. McKenna, L.L. Wright, D.J. Miller, G. Glatzmeier, J. Am. Chem. Soc. 101 (1979) 5245;
(b) M. McKenna, L.L. Wright, D.J. Miller, L. Tanner, R.C. Haltiwanger, M. Rakowski DuBois, J. Am. Chem. Soc. 105 (1983) 5329.
[10] (a) C.J. Casewit, M. Rakowski DuBois, J. Am. Chem. Soc. 108 (1986) 5482;
(b) Y. Nishibayashi, I. Wakiji, K. Hirata, M. Rakowski DuBois, H. Hidai, Inorg. Chem. 40 (2001) 578.
[11] C.J. Casewit, J.R. Dunkle, M. Rakowski DuBois, C.M. Elliott, J. Electrochem. Soc. 136 (1989) 1040.
[12] (a) F. Maseras, A. Lledòs, E. Clot, O. Eisenstein, Chem. Rev. 100 (2000) 601;
(b) G.J. Kubas, Adv. Inorg. Chem. 56 (2004) 127.
[13] T.B. Rauchfuss, Inorg. Chem. 43 (2004) 14.
[14] (a) D.L DuBois, W.K. Millar, M. Rakowski DuBois, J. Am. Chem. Soc. 103 (1981) 3429;
(b) D.L. DuBois, F. Kvietok, M. Rakowski DuBois, Inorg. Chem. 32 (1993) 561;
(c) W. Tremel, R. Hoffmann, E.D. Jemmís, Inorg. Chem. 28 (1989) 1213.
[15] (a) S. Blasco, I. Demachy, Y. Jean, A. Lledos, New. J. Chem. 25 (2001) 611;
(b) S.Z. Knottenbelt, J.E. McGrady, J. Am. Chem. Soc. 125 (2003) 9846;
(c) J.-M. Mouesca, J.L. Chen, L. Noodleman, D. Bashford, D.A. Case, J. Am. Chem. Soc. 116 (1994) 11898;
(d) J. Li, M.R. Nelson, C.Y. Peng, D. Bashford, L. Noodleman, J. Phys. Chem. A 102 (1998) 6311.
[16] (a) J.W. Tye, M.B. Hall, I.P. Georgakaki, M.Y. Darensbourg, Adv. Inorg. Chem. 56 (2004) 1;
(b) P.E.M. Siegbahn, Adv. Inorg. Chem. 56 (2004) 101.
[17] (a) T. Lovell, J. Li, T. Liu, D.A. Case, L. Noodleman, J. Am. Chem. Soc. 123 (2001) 12392;
(b) T. Lovell, J. Li, D.A. Case, L. Noodleman, J. Am. Chem. Soc. 125 (2003) 8377;
(c) T. Lovell, J. Li, D.A. Case, L. Noodleman, J. Am. Chem. Soc. 124 (2002) 4546;
(d) T. Lovell, R.A. Torres, W.-G. Han, T. Liu, D.A. Case, L. Noodleman, Inorg. Chem. 41 (2002) 5744;
(e) T. Lovell, J. Li, D.A. Case, L. Noodleman, J. Biol. Inorg. Chem. 7 (2002) 735;
(f) L. Noodleman, T. Lovell, W.-G. Han, J. Li, F. Himo, Chem. Rev. 104 (2004) 459.
[18] A. Ienco, M.J. Calhorda, J. Reinhold, F. Reineri, C. Bianchini, M. Peruzzini, F. Vizza, C. Mealli, J. Am. Chem. Soc. 126 (2004) 11954.
[19] R.G. Parr, W. Yang, Density Functional Theory of Atoms and Molecules, Oxford University Press, Oxford, UK, 1989.
[20] T. Ziegler, Chem. Rev. 91 (1991) 651.
[21] M.J. Frisch, G.W. Trucks, H.B. Schlegel, G.E. Scuseria, M.A. Robb, J.R. Cheeseman, J.A. Montgomery Jr., T. Vreven, K.N. Kudin, J.C. Burant, J.M. Millam, S.S. Iyengar, J. Tomasi, V. Barone, B. Mennucci, M. Cossi, G. Scalmani, N. Rega, G.A. Petersson, H. Nakatsuji, M. Hada, M. Ehara, K. Toyota, R. Fukuda, J. Hasegawa, M. Ishida, T. Nakajima, Y. Honda, O. Kitao, H. Nakai, M. Klene, X. Li, J.E. Knox, H.P. Hratchian, J.B. Cross, V. Bakken, C. Adamo, J. Jaramillo, R. Gomperts, R.E. Stratmann, O. Yazyev, A.J. Austin, R. Cammi, C. Pomelli, J.W. Ochterski, P.Y. Ayala, K. Morokuma, G.A. Voth, P. Salvador, J.J. Dannenberg, V.G. Zakrzewski, S. Dapprich, A.D. Daniels, M.C. Strain, O. Farkas, D.K. Malick, A.D. Rabuck, K. Raghavachari, J.B. Foresman, J.V. Ortiz, Q. Cui, A.G. Baboul, S. Clifford, J. Cioslowski, B.B. Stefanov, G. Liu, A. Liashenko, P. Piskorz, I. Komaromi, R.L. Martin, D.J. Fox, T. Keith, M.A. Al-Laham, C.Y. Peng, A. Nanayakkara, M. Challacombe, P.M.W. Gill, B. Johnson, W. Chen, M.W. Wong, C. Gonzalez, J.A. Pople, GAUSSIAN 03, Gaussian, Inc., Wallingford, CT, 2004.
[22] (a) C. Lee, W. Yang, R.G. Parr, Phys. Rev. B 38 (1988) 785;
(b) A.D. Becke, J. Chem. Phys. 98 (1993) 5648.
[23] (a) W.R. Wadt, P.J. Hay, J. Chem. Phys. 82 (1985) 284;
(b) T.H. Dunning Jr., P.J. Hay, in: H.F. Schaefer (Ed.), Modern Theoretical Chemistry, Plenum Press, New York, 1976, pp. 1–28.
[24] A.W. Ehlers, M. Böhme, S. Dapprich, A. Gobbi, A. Höllwarth, V. Jonas, K.F. Köhler, R. Stegmann, A. Velokamp, G. Frenking, Chem. Phys. Lett. 208 (1993) 111.
[25] A.W. Ehlers, M. Böhme, S. Dapprich, A. Gobbi, A. Höllwarth, V. Jonas, K.F. Köhler, R. Stegmann, A. Velokamp, G. Frenking, Chem. Phys. Lett. 208 (1993) 237.